ELSEVIER

Biochimica et Biophysica Acta 1236 (1995) 31–38

BBA Biochimica et Biophysica Acta

Molecular mechanism for the relative binding affinity to the intestinal peptide carrier. Comparison of three ACE-inhibitors: enalapril, enalaprilat, and lisinopril

Peter W. Swaan *, Marco C. Stehouwer, Josef J. Tukker

Department of Pharmaceutics, Utrecht Institute of Pharmaceutical Sciences (UIPS), University of Utrecht, Utrecht, The Netherlands

Received 23 September 1994; accepted 23 January 1995

Abstract

The affinity of three substrates for the intestinal peptide carrier is explained based on their three-dimensional (3D) structural data. The kinetic transport parameters of three ACE-inhibitors, enalapril, enalaprilat, and lisinopril, have been determined in an in vitro system using rat intestine. The observed kinetic transport parameters (±asymptotic standard error) of enalapril are: 0.81 (±0.23) mM, 0.58 (±0.37) μmol/h per cm^2, and 0.56 (±0.04) cm/h for the half-maximal transport concentration (K_T), the maximal transport flux (J_{max}) and the passive permeability constant (P_m). Enalaprilat was transported by passive diffusional with a P_m of 0.51 (±0.04) cm/h. For lisinopril the kinetic transport parameters were 0.38 (±0.19) mM, 0.12 (±0.07) μmol/h per cm^2, and 0.18 (±0.02) cm/h for K_T, J_{max}, and P_m, respectively. The affinity of the ACE-inhibitors for the intestinal peptide carrier has been evaluated based on their ability to inhibit the transport rate of cephalexin. The inhibition constants (K_i) of enalapril, enalaprilat and lisinopril were 0.15, 0.28 and 0.39 mM, respectively. 3D structural analysis of lisinopril using molecular modelling techniques reveals that intramolecular hydrogen bond formation is responsible for decreased carrier affinity.

Keywords: Intestinal transport; Peptide transporter; Structure–transport relation; Computational chemistry

1. Introduction

Di- and tripeptides and their structural analogues are actively transported into the intestinal epithelial cells by a specific carrier system that is different from those involved in the transport of amino acids [1]. Recent studies in various in vitro and in vivo models provided more insight in the wide range of compounds that show affinity for the peptide transporter. Among these compounds are several β-lactam antibiotics, such as cephalosporins and penicillins, and angiotensin converting enzyme (ACE) inhibitors [2]. However, there seems to be little knowledge about the specific structural requirements necessary for recognition by the peptide carrier proteins. It was hypothesised previously that the minimal spatial requirements for binding to the peptide carrier consists of a free carboxylic acid moiety and an amide bond [3–5]. The molecular binding sites, however, are still unknown, although recently advances have been made by photo-affinity labelling of the carrier using benzylpenicillin [6] and attempts have been made to clone the intestinal peptide carrier [7,8]. Recently, expression cloning of the peptide carrier from rabbit small intestine in *Xenopus laevis* has led to the description of the primary structure of this membrane protein [9]. Further isolation and purification of the carrier proteins and subsequent X-ray crystallography or three-dimensional (3D)-NMR studies may provide the secondary to quaternary structures of this protein and might lead to more insight into the real spatial requirements of the peptide carrier. Until then, a deeper understanding of the structural requirements of this carrier can only be obtained from in vitro studies and indirect molecular modelling approaches. In this study an attempt is made to explain the observed differences in affinity for the carrier by comparing the 3D structural features of three

Abbreviations: ACE, angiotensin converting enzyme; CFX, cephalexin.

* Corresponding author. Present address: Department of Pharmacy and Pharmaceutical Chemistry, P.O. Box 0446, University of California, San Francisco, CA 94143-0446, USA. Fax: +1 (415) 4760688. E-mail: swaan@itsa.ucsf.edu.

SSDI 0005-2736(95)00030-5

potential substrates: enalapril, enalaprilat and lisinopril, which are structurally closely related to each other (Fig. 1). The transport of the two ACE-inhibitors lisinopril and enalapril in rats has been shown to be a combination of both passive and active processes, involving the carrier-mediated peptide transport system [10,11].

Enalapril is an ester prodrug of the pharmacologically active enalaprilat. Following oral administration of enalapril, the parent compound (enalaprilat) is formed by bioconversion of enalapril. Enalaprilat, a diacid, binds slowly and tightly to ACE, producing well-defined clinical effects, but is poorly absorbed from the gastrointestinal tract (3–12% bioavailability) [12]. The prodrug approach of esterifying enalaprilat to enalapril is required in order to enhance the oral bioavailability to 60–70% [1].

Lisinopril is a structural homologue of enalaprilat, differing only in the second amino acid side chain (Fig. 1). Lisinopril inhibits ACE in vitro, as well as after parenteral and oral administration to humans; its oral bioavailability is only 25–29%, but it has a longer duration of action than enalapril [13].

The octanol-water distribution coefficients (D) of several ACE-inhibitors were recently studied by Ranadive et al. [14] in an attempt to correlate lipophilicity with reported data for oral absorption. They reported a $\log D$ lower than -3 for enalaprilat and lisinopril at pH 7, while enalapril has a $\log D$ of -1.2.

In this paper the transport parameters of these three structurally related compounds and their ability to competitively inhibit the transport of cephalexin, a known substrate for the intestinal peptide carrier [15–17], was studied in rat intestinal tissue in vitro. The analysis might lead to a better understanding of the structure–absorption relationship for active transport by the small intestinal peptide carrier system.

2. Materials and methods

2.1. Materials

Enalapril maleate and cephalexin were obtained from Sigma (Brussels, Belgium). Lisinopril and enalaprilat were a kind gift of Merck (Rahway, NJ). All other chemicals were of analytical grade.

2.2. In vitro intestinal transport studies

Transport of cephalexin (CFX), enalapril, enalaprilat and lisinopril across living intestinal tissue was performed by using custom-built Ussing chambers. Rat intestine was obtained from male Wistar rats (U:WU; 200–250 g) which had access to a standard laboratory chow and tap water prior to experiments. After decapitation and laparotomy, the small intestine (starting 20 cm proximal to the ileocaecal junction) was quickly excised and placed into an ice-cold Tris-Ringer solution containing (mM): Na^+, 134.0; K^+, 5.0; Ca^{2+}, 1.2; Mg^{2+}, 1.2; Cl^-, 118.8; HCO_3^-, 25.0; and Tris, 7.4. The intestine was stripped of its underlying muscle layer, placed between two Lucite® chambers (1.0 cm^2 exposed tissue surface), and bathed on both sides with a Tris-Ringer solution containing 10 mM glucose on the serosal and 10 mM mannitol on the mucosal side. Respective to rat body temperature, bathing solutions were kept at 38° C [18] by using thermostated water-jackets. During transport studies, tissue integrity was validated by measuring the permeability across the intestinal tissue of a fluorescent transport marker, Lucifer yellow CH. Tissue viability was checked by monitoring the electrical parameters of the tissues as described previously [19].

After a 45 min equilibration time, CFX, enalapril, enalaprilat or lisinopril was added to the mucosal side of the membrane and 200 μl samples were taken from serosal compartments at 30 min intervals up to 210 min. To maintain a constant volume, 200 μl of Tris-Ringer solution containing 10 mM glucose was replaced after each sample. Effect of compound withdrawal was taken into account for when calculating the fluxes. Backflux was neglected since it never exceeded 1% of the mucosal-to-serosal flux. The concentrations studied were 0.1, 0.3, 0.5, 1, 2, 3, and 5 mM for all ACE-inhibitors and 0.1, 0.3, 0.5, 1, 3, and 10 mM for CFX.

2.3. Inhibition studies

Inhibition of CFX transport by enalapril, enalaprilat and lisinopril was performed at various concentrations of CFX. The mucosal-to-serosal (m-to-s) flux of 0.3, 0.5, 1, 3 and 5 mM CFX was monitored for 90 min, then enalapril, enalaprilat or lisinopril (1 mM) was added to the mucosal side of the membrane. After a 30 min incubation period the CFX flux was monitored for another 90 min.

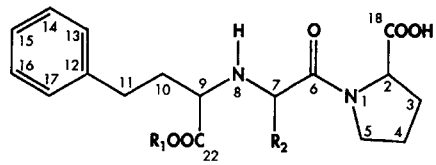

	R_1	R_2
Enalapril	$-C_2H_5$	$-CH_3$
Enalaprilat	$-H$	$-CH_3$
Lisinopril	$-H$	$-(CH_2)_4NH_2$

Fig. 1. Chemical structures of the ACE-inhibitors enalaprilat, enalapril, and lisinopril. For clarity, only hydrogen atoms attached to hetero-atoms are shown. The nitrogen atom in the lysyl (R_2) side chain of lisinopril has atom number 29.

2.4. Analytical procedures

Enalapril, enalaprilat and lisinopril were determined by isocratic reversed-phase HPLC using a Waters QA-1 system (Waters Associates, Millford, MA) with two built-in UV detection units operating at 230 and 254 nm. A Waters NovaPak® C18 column (3.9 × 150 mm; 4 μm particles) was used at room temperature with a freshly degassed and filtered (Millipore 0.22 μm) mixture (v/v) of 20% methanol and 80% 10 mM KH_2PO_4 which had a pH of 5. The flow rate was 1.0 ml/min. The retention times of enalapril, enalaprilat and lisinopril were 3.0, 6.5 and 13.0 min, respectively. CFX was analysed with an HPLC system consisting of a Waters 6000A pump, a Kratos Spectroflow 773 variable wavelength UV detector operating at 220 nm, and a WISP model 710B autosampler unit. The column was a Merck LiChrospher 100 RP-18 (5 μm) with a LiChrocart 4-4 (LiChrosorb RP-18; 5 μm) guard column. The same eluent was used as described above for the ACE-inhibitor analyses. The retention time of CFX on this system was 7.0 min. The injection volume was 50 μl for all samples. Lucifer yellow was analysed on a Perkin Elmer luminescence spectrometer LS50 (Perkin Elmer, Buckinghamshire, UK) fixed at an excitation wavelength of 428 nm (slid width 2.5 nm) and an emission wavelength of 540 nm (slid width 10 nm).

2.5. Transport data analysis

The observed transmembrane flux data were screened for the possible involvement of a carrier-mediated transport component. The general expression for such a mixed active/passive intestinal transport mechanism is best described by:

$$J_{tot} = J_{act} + J_{pass} \quad (1)$$

where J_{tot} represents the total flux of a compound measured and J_{act} and J_{pass} represent the active and passive component, respectively, which are defined as:

$$J_{act} = \frac{J_{max} C}{K_T + C} \quad (2)$$

and:

$$J_{pass} = P_m C \quad (3)$$

where J_{max} is the maximal carrier flux, C the concentration of the studied compound at the donor side, K_T the concentration at half-maximal flux resembling the Michaelis-Menten constant, and P_m the passive permeability constant, thus resulting in:

$$J_{tot} = \frac{J_{max} C}{K_T + C} + P_m C \quad (4)$$

Eqs. (3) and (4) are fitted to the observed data sets using a regular least-squares fitting program for Eq. (3) and the NONLIN module in SYSTAT [20] for solving Eq. (4). Initial numeric estimates of the kinetic transport parameters in NONLIN are computed using the Quasi-Newton algorithm. The resulting r^2 values for each compound using both equations gives a good indication whether the transport process of a compound is either a linear (passive) or a non-linear (mixed active/passive) process over concentration.

If the concentration of the solute is much lower than K_T, Eq. (4) can be modified to:

$$J_{tot} = P_c C + P_m C \quad (5)$$

where P_c, or carrier permeability, is defined as the ratio of J_{max} and K_T. Comparison of P_c with P_m can give a relative indication of the fraction of a solute transported by either carrier-mediated or passive transport.

In inhibition studies the total CFX flux data in presence and absence of inhibitors were corrected for the passive transport component ($P_m C$). Eq. (2) was fitted to the resulting data to obtain transport parameters of CFX in absence and presence of inhibitors. In order to obtain the kinetic inhibition constant of the inhibitors Eq. (2) was modified to:

$$\frac{1}{J_{act}} = \frac{1}{J_{max}} + \left(\frac{K_T}{J_{max}}\right)\left(1 + \frac{[I]}{K_i}\right)\left(\frac{1}{C}\right) \quad (6)$$

where [I] represents the concentration of the inhibitor and K_i the inhibition constant. A double reciprocal plot of J_{act} versus C yields a straight line (Lineweaver-Burk plot) with intercept $1/J_{max}$. K_i is calculated from the change in slope in the presence of inhibitor relative to the slope in the absence of inhibitor. This change in slope is equal to the term $(1 + ([I]/K_i))$.

2.6. Computational chemistry

Molecular mechanical calculations were performed with the programme Chem3D Plus™ [21], mounted on an Apple Macintosh IIcx or SE/30 model computer. Energy minimisations were carried out using the TINKER minimiser [22]. Semi-empirical calculations were performed on a Silicon Graphics Iris Crimson Elan workstation using MOPAC with the AM1 Hamiltonian [23]. The crystal structure of lisinopril was used to provide starting coordinates in the calculations [24]. This crystal structure represents the conformation of a neutral molecule. Since lisinopril is protonated at physiological pH, hydrogen atoms were removed from the two carboxyl moieties and a hydrogen atom was added to the nitrogen of the lysyl side chain at standard bond lengths and angles before further calculations were performed. The protonated structure was initially refined by molecular mechanical energy minimisation in vacuo, excluding electrostatic interactions, and atomic point charges were calculated from this first set of refined structures. The subsequent MOPAC calculations

included the keywords PRECISE, EF, MMOK, NOINTER and CHARGE = −1 to account for the net negative charge of the molecule.

Molecular dynamics simulations were carried out with Chem3D Plus™ using the Beeman algorithm [25], with a dynamics step interval of 1.0 fs, a heating/cooling rate of 4.2 kJ/atom per ps, and a target temperature of 300 K. An equilibration time of 5 ps was run in order to reach the target temperature. After reaching the target temperature, the run was continued for 25 ps and new conformations were stored every 50 fs. Intramolecular distances between oxygen atoms O(10) to O(13), carbon atoms C(18) and C(22), and nitrogen atom N(29) were calculated for each conformation and stored in a database.

There is one important limitation to the accuracy of our dynamics computations. The calculations do not take water molecules into account. Ignoring the solvent could, among other consequences, cause the structures to appear more flexible than they are in reality. The addition of solvent to the calculations would, however, increase the computation time beyond feasible limits on our systems.

3. Results

3.1. Intestinal transport: concentration dependency of transport

Transport of the ACE-inhibitors enalapril, enalaprilat and lisinopril was measured over the concentration range up to 5 mM. Fig. 2 shows the relation between the mucosal concentration of enalapril and enalaprilat and their respective transmembrane flux. Eq. (4) is best fitted to the observed data for enalapril (corrected [1] r^2 0.994), whereas enalaprilat is best described by a straight line (corrected r^2 0.432 after fitting Eq. (4) and 0.983 after fitting Eq. (3) to the data set). Fig. 3 shows the plot of the relationship between concentration and the observed flux for lisinopril. The observed transport rates show a non-linear relationship with concentration at the concentrations studied. Therefore, the involvement of a carrier-mediated transport process is suspected. Eq. (4) gives an excellent description of experimental data from lisinopril with a corrected r^2 of 0.985. The two transport components J_{pass} and J_{act}, which both constitute the total flux J_{tot} are visualised in the picture for clarity. The calculated transport parameters are given in Table 1.

The solid lines in Figs. 2 and 3 which represent J_{tot} for enalapril and lisinopril, respectively, were generated using the parameters derived from non-linear regression of the observed data with Eq. (4). The obtained values of J_{max}, K_T, P_m, and P_c are listed in Table 1.

The intestinal transport mechanism of CFX was studied in addition to its use in inhibition experiments. Fig. 4 shows the non-linear concentration dependent behaviour of CFX in Ussing chambers. Eq. (4) was used to fit the straight line to the observed data. The resulting kinetic transport parameters are given in Table 1.

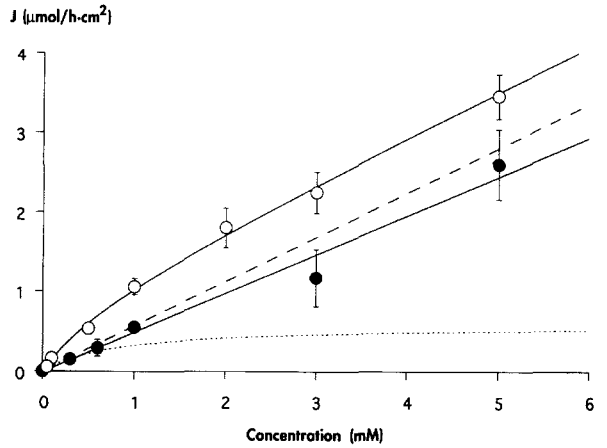

Fig. 2. Concentration dependent transport of enalapril and enalaprilat. Rat small intestinal tissue was placed in Ussing chambers at 38° C. At $t = 0$ enalapril (open circles) or enalaprilat (closed circles) was added to the mucosal bathing solution and their transport across the intestinal epithelia was followed by measuring the concentration on the serosal side of the membrane ($n \geq 3$ ±S.D.). The solid lines represent the estimated J_{tot} for enalapril and enalaprilat calculated by substituting the estimated transport parameters from Table 1 in Eqs. (3) and (4), respectively. The dashed and dotted lines represent the passive and active transport components of enalapril, respectively.

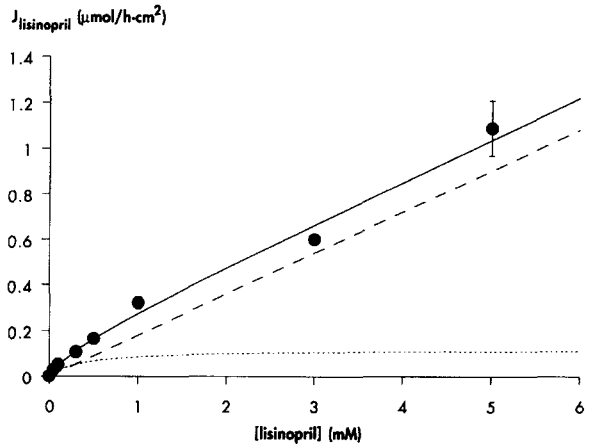

Fig. 3. Concentration-dependent transport of lisinopril. Rat small intestinal tissue was placed in Ussing chambers at 38° C. At $t = 0$ lisinopril was added to the mucosal bathing solution and the amount transported to the serosal bathing solution was analysed ($n = 3$ or 4 ±S.D.). The solid, dashed and dotted lines represent J_{tot}, J_{pass} and J_{act}, respectively, and were generated from Eq. (4), using the SYSTAT fitted parameters listed in Table 1. Error bars smaller than the corresponding data points are not visible.

[1] Corrected for the proportion of the variable in the dependent variable reduced to a level expected when using this model in a new sample from the same population.

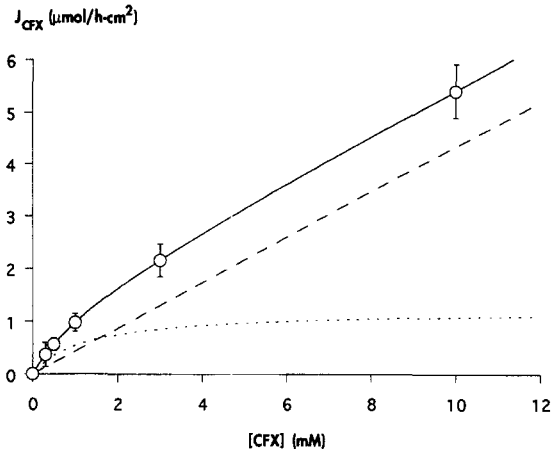

Fig. 4. Concentration-dependent transport profile of CFX in rat intestine. CFX was added to the mucosal side of rat small intestinal membrane mounted in Ussing chambers at 38° C. The results are presented as means (±S.D.) of three or more experiments. J_{tot}, J_{pass} and J_{act} are represented by solid, dashed and dotted lines, respectively.

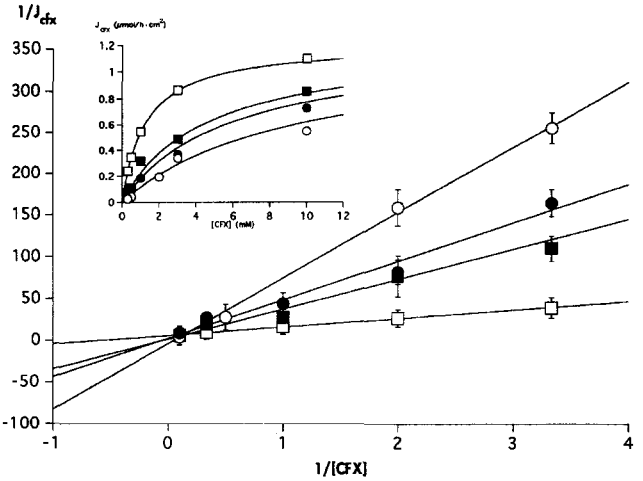

Fig. 5. Lineweaver-Burk plot of CFX inhibition by three ACE-inhibitors. CFX transport over rat small intestinal tissue was followed in Ussing chambers. After a control period of 90 min (open squares), 1 mM lisinopril (closed squares), enalaprilat (closed circles) or enalapril (open circles) was added to the mucosal side of the membrane and the CFX was measured for another 90 min period. The values are corrected for non-carrier-mediated carrier transport. The straight lines are calculated by weighted least-squares regression ($n = 3$ or 4 ±S.D.). The inset figure represents the same data on a linear scale. J_{CFX} in μmol/h per cm² and [CFX] in mM.

3.2. Inhibition studies

Transport of CFX was determined in the absence and presence of enalapril, enalaprilat and lisinopril over a concentration range of 0.3 to 5 mM. The Lineweaver-Burk plots of CFX transport in the absence or presence of the three ACE-inhibitors after correction for the passive diffusion component of CFX is illustrated in Fig. 5. The inset in Fig. 5 shows that lisinopril, enalapril and enalaprilat cause an increase in the apparent K_T for CFX without altering J_{max}, indicating a competitive inhibition process and sharing of the same transport carrier. The apparent K_T value of CFX was 9.42, 5.62 and 4.38 in the presence of enalapril, enalaprilat and lisinopril, respectively. The calculated values for the inhibition constant, K_i, are shown in Table 1.

3.3. Molecular modelling

Fig. 6 shows the structure of lisinopril after optimisation by MOPAC. Optimisation has placed the lysyl side chain amid the two carboxylate moieties. The dotted lines represent the possible hydrogen bonds between the ammonium hydrogen atoms and the carboxylate oxygen atoms. The intramolecular distance between the oxygen atoms and the nitrogen atom was measured and the results are presented in Table 2.

Fig. 7 shows a molecular dynamics run of 30 ps starting with the crystallographic structure of lisinopril. The starting structure reveals close proximity between the lysyl side chain nitrogen atom N(29) and the carboxylate carbon atom C(18). After reaching the target temperature at approx. 4 ps a dramatic decrease in the distance between C(22) and N(29) is observed. During the remainder of the run, the lysyl side chain alternates more or less equally between the two carboxylate groups. Considering the hydrogen bond cut-off distance of approx. 3 Å for an N^+-

Table 1
Calculated kinetic transport parameters and inhibition constants for three ACE-inhibitors and CFX [a]

	Enalapril	Enalaprilat	Lisinopril	CFX
K_T (mM) [b]	0.81 (0.23)	–	0.38 (0.19)	1.23 (0.62)
J_{max} (μmol/h per cm²) [c]	0.58 (0.37)	–	0.12 (0.07)	1.21 (0.37)
P_c (cm/h) [d]	0.72 (0.43)	–	0.32 (0.20)	0.98 (0.72)
P_m (cm/h) [e]	0.56 (0.04)	0.51 (0.04)	0.18 (0.02)	0.43 (0.03)
K_i (mM) [f]	0.15	0.28	0.39	

[a] Parameters were calculated by non-linear regression to Eq. (4). Values in parentheses are asymptotic standard errors; parameters are based on seven different concentration points of each compound, each concentration point comprises the results of 4 to 8 animals.
[b] Half-maximal concentration.
[c] Maximal carrier flux.
[d] Carrier permeability.
[e] Passive permeability coefficient.
[f] Inhibition constant.

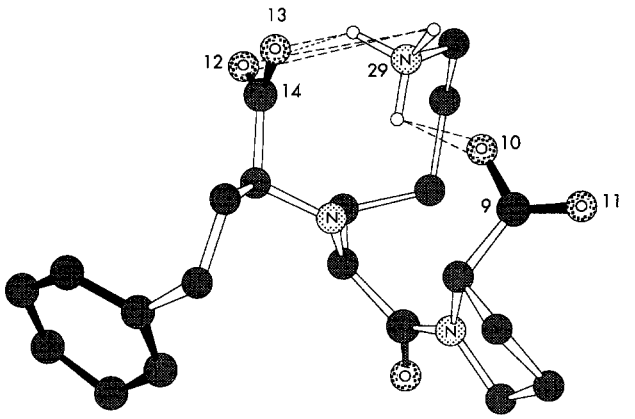

Fig. 6. Three-dimensional representation of lisinopril after geometrical optimisation by MOPAC. All hetero-atoms and functional groups are shown (gray circles represent carbon atoms; gray bonds represent sp^2 hybridisation); for clarity only hydrogen atoms on N(29) are shown. Dotted lines represent hydrogen bonds.

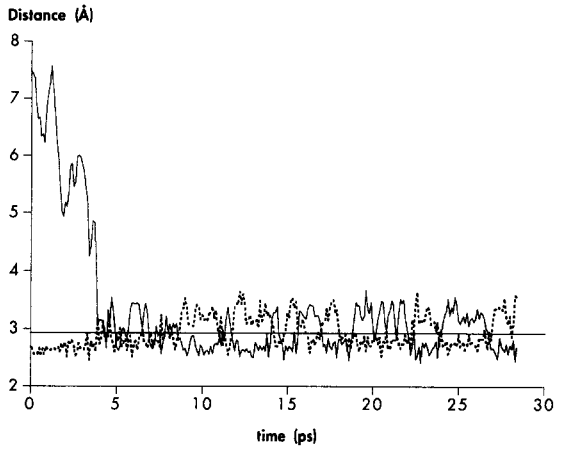

Fig. 7. Molecular dynamics simulation of lisinopril. The observed intramolecular distance between lysyl nitrogen atom (N(29)) and the two carboxylate carbon atoms is plotted against time (C(18): dotted line; C(22): straight line). The horizontal straight line at approx. 3 Å represents the cut-off distance for hydrogen bond formation.

H · · · O system, it was calculated that the lysyl side chain points in the direction of, and is liable to form hydrogen bonds with, the C(18) carboxylate group in 44% of the sampled conformations, while 56% of the conformations show a preferred interaction with the C(22) moiety. This suggests that the lysyl side chain slightly favours an interaction with the C(22) carboxylic acid function by formation of a hydrogen bond.

4. Discussion

The intestinal peptide transporter has a broad substrate specificity. Among its substrates are members of different pharmaceutically relevant drug groups such as the ACE-inhibitors and β-lactam antibiotics. For this reason, the transporter has been recognised as an important intermediate in the bioavailability of these compounds. However, the lack of knowledge regarding structural specificity towards its substrates has prevented the use of this transporter on a more rational basis. Our objective was to study the transport mechanism of three structurally related compounds that have affinity for the peptide transporter and to explain the difference in their carrier affinity by comparing the difference in their 3D structural features using molecular modelling techniques. The intestinal transport mechanisms of the three ACE-inhibitors, enalapril, enalaprilat and lisinopril, was studied in an in vitro transport system using rat intestine. Fig. 2 shows the transepithelial transport rates of enalapril and enalaprilat over concentration. Enalapril shows an apparent non-linear concentration dependent behaviour, indicating the involvement of a carrier-mediated transport mechanism. The parent compound of enalapril, enalaprilat, lacks an ethyl ester group at the C(22) position (Fig. 1) and therefore carries a double negative charge at a physiological pH. Enalaprilat shows a linear concentration dependent transport mechanism (Fig. 2), which indicates that this compound traverses the intestinal epithelium using a passive pathway. More evidence for a passive transport mechanism of enalaprilat was provided by the fact that polarity in enalaprilat transport direction was not observed (data not shown). Considering the slight difference in the molecular structure of enalaprilat and its ester prodrug enalapril, it becomes evident that the double negative charge prevents enalaprilat from using a carrier-mediated transport pathway for its transepithelial transfer. From Table 1 it can be noted that the passive permeability constant (P_m) of enalapril and enalaprilat are not significantly different (t-test; $P < 0.05$). From this observation it would be expected that the lipophilicity of both compounds should be nearly equal if the passive transport process is totally transcellular. However, enalaprilat has a $\log D < -3$ while its ethyl ester prodrug enalapril has an observed $\log D$ of -1.2 [13]. This extremely low lipophilicity of enalaprilat is not surprising with respect to its double negative charge. Accordingly, the difference in lipid solubility does not account for the observed equality in P_m. Therefore, the observed passive transport rate of enalaprilat cannot be explained by a transcellular transport mechanism alone. This problem still remains to be addressed.

Table 2
Intramolecular distances between hydrogen bond donors and acceptors in lisinopril after optimisation with MOPAC

Hydrogen bond donor · · · acceptor	Distance (Å)
N(29) · · · O(10)	4.45
N(29) · · · O(11)	2.35
N(29) · · · O(15)	2.86
N(29) · · · O(16)	2.78

CFX is known to be transported by the intestinal peptide carrier [26,27]. Fig. 4 and Table 1 show that the transport of CFX in rat intestine is a non-linear concentration dependent process, which is in agreement with the accepted transport mechanism for this compound. The transport of CFX in presence of the three ACE-inhibitors was used to calculate the relative affinity of these compounds for the peptide transporter. Fig. 5 reveals that all three ACE-inhibitors are capable of competitively inhibiting CFX transport, indicating that they share a common affinity for the peptide carrier. The calculated inhibition constants (K_i) reveal that enalapril has the highest affinity for the peptide transporter (Table 1). It is interesting to note that enalaprilat, which is not transported by the peptide transporter, nevertheless shows affinity for this carrier. Presumably, enalaprilat binds to the peptide transporter, hence its capability to inhibit CFX transport, but is not transported to the other side of the intestinal membrane. This can be explained by a difference in the molecular structure of these two compounds which causes them to be both recognised by the carrier system but prevents enalaprilat from being transported. As mentioned earlier, the only difference between enalapril and its parent compound on a molecular level is an ester function on enalaprilats C(22) carboxylic acid group (Fig. 1). It was hypothesised previously [4] that a free endstanding carboxylic acid group is essential for recognition by the peptide carrier. Therefore, the second negative group in enalaprilat must have a negative influence on the transepithelial transport process but not on binding with the transporter. This phenomenon has also been observed with other pairs of ACE-inhibitor and β-lactam drug/prodrugs, where the parent compound or pharmacologically active drug has a double negative charge and its orally available ester prodrug has only one free carboxylate group at the C(18) position, e.g., quinapril and quinaprilat, ramipril and ramiprilat, carfecillin and carbenicillin [28].

Summarising, the lower K_i of enalapril in respect to enalaprilat indicates a greater affinity for the peptide carrier which can be explained by a higher affinity of the ester group for the binding site on the peptide carrier proteins, or by a higher repulsion interaction between the peptide carrier and the negatively charged C(22) carboxylic acid group in enalaprilat. Moreover, both observations indicate the possible existence of an extra, thus far unknown interaction site on the intestinal peptide transporter, which is supplementary to the pharmacophore as described previously [3].

Lisinopril transport through rat intestine appears to be a non-linear concentration dependent process. Fig. 3 shows that a carrier-mediated transport mechanism is involved in the transepithelial transport of lisinopril. Despite the fact that lisinopril has a second free carboxylic moiety on the C(22) position (Fig. 1), it clearly shows carrier-mediated transepithelial transport. This is in contrast with enalaprilat, which only shows affinity to the carrier but no carrier-mediated transport. Examination of the differences in molecular homology cannot provide a satisfactory explanation for the observed affinity of lisinopril for the peptide transporter. Therefore, the molecular structure of this compound was studied with molecular modelling tools. Three-dimensional in computro analysis of the structure of lisinopril (Fig. 6) reveals that the lysyl side chain favours to form hydrogen bonds with the C(22) carboxylate group. In that way, the lysyl side chain is likely to shield the unfavourable interaction of the negative C(22) carboxylic moiety with the peptide transporter. Table 1 shows that the affinity of lisinopril for the peptide carrier is almost three times lower than the affinity of enalapril for the same transporter. This can be explained by the fact that the lysyl side chain not only forms hydrogen bonds with the C(22) carboxylic acid, but also with the endstanding C(18) carboxylic acid moiety (Figs. 6 and 7), which is essential for recognition by the peptide carrier. The observed lower affinity for the peptide carrier is in good agreement with previous studies [3], where it was assumed that affinity for the intestinal peptide transporter can be diminished or abolished by structural hindrance of the endstanding free carboxylic acid moiety. The combined results of Figs. 6 and 7 suggest that a considerable amount of the time (approx. 40%) the C(18) carboxylic acid group is blocked by the charged lysyl side chain. From the transport data it is obvious that the K_T as well as the P_c of lisinopril are both half the value of their respective parameters for enalapril. The observed differences in both the carrier permeability, P_c, and the half-maximal concentration, K_T, which can be loosely interpreted as the affinity for the carrier [29], are in good agreement with the observed differences in 3D structure between enalapril and lisinopril.

In conclusion, we have shown in this study that comparison of the three-dimensional structure of substrates for a specific transporter can reveal valuable information about the actual mechanism of substrate affinity and subsequent transport. It was shown that it is possible to explain differences in transport behaviour in vitro based on structural data. The presented data form additional evidence for the fundamental need of a free endstanding carboxylate moiety on a substrate for the peptide carrier and the adverse effect of a double negative charge on the transportability of this substrate. Therefore, this study provides additional insight to our existing knowledge about the structural requirements for recognition and transport by the intestinal peptide transporter.

References

[1] Iseki, K., Sugawara, M., Saitoh, H., Miyazaki, K. and Arita, T.J. (1989) Pharm. Pharmacol. 41, 628–632.
[2] Sinko, P.J., Hu, M., and Amidon, G.L. (1987) Adv. Drug Del. Systems 3, 115–121.

[3] Swaan, P.W. and Tukker, J.J. (1991) Pharm. Res. 8, S127.
[4] Swaan, P.W. and Tukker, J.J. (1992) Pharm. Res. 9, S180.
[5] Swaan, P.W. (1993) Prodrug targeting to the intestinal peptide carrier, pp. 123–143, Thesis, University of Utrecht, Utrecht.
[6] Kramer, W., Girbig, F., Leipe, I. and Petzoldt, E. (1989) Biochem. Pharmacol. 37, 2427–2435.
[7] Miyamoto, Y., Thompson, Y.G., Howard, E.F., Ganapathy, V. and Leibach, F.H. (1991) J. Biol. Chem. 266, 4742–4745.
[8] Saito, H., Ishii, T. and Inui, K.-I. (1993) Biochem. Pharmacol. 45, 776–779.
[9] Fei, Y.-J., Kanai, Y., Nussberger, S., Ganapathy, V., Leibach, F.H., Romero, M.F., Singh, S.K., Boron, W.F. and Hediger, M.A. (1994) Nature 368, 563–566.
[10] Friedman, D.I. and Amidon, G.L. (1989) J. Pharm. Sci. 78, 995–998.
[11] Friedman, D.I. and Amidon, G.L. (1989) Pharm. Res. 6, 1043–1047.
[12] Kubo, S.H. and Cody, R.J. (1985) Clin. Pharmacokinetics 10, 377–391.
[13] Lancaster, S.G. and Todd, P.A. (1988) Drugs 35, 646–669.
[14] Ranadive, S.A., Chen, A.X. and Serajuddin, A.T.M. (1992) Pharm. Res. 9, 1480–86.
[15] Dantzig, A.H. and Bergin, L. (1990) Biochim. Biophys. Acta 1027, 211–217.
[16] Dantzig, A.H. and Bergin, L. (1988) Biochem. Biophys. Res. Commun. 155, 1082–1087.
[17] Yamashita S., Yamazaki, Y., Mizuno, M., Masada, M., Nadai, T., Kimura, T. and Sezaki, H. (1984) J. PharmacobioDyn. 7, 227–233.
[18] Davies, B. and Morris, T. (1993) Pharm. Res. 10, 1093–1095.
[19] Swaan, P.W., Marks, G.J., Ryan, F.M. and Smith, P.L. (1994) Pharm. Res. 11, 283–287.
[20] SYSTAT (1989) Evanston.
[21] Chem3D Plus™ (1989–1993) The molecular modeling system, version 3.1.1, Cambridge Scientific Computing, Cambridge.
[22] Ponder, J.W. and Richards, F.M. (1987) J. Comp. Chem. 8, 1016–1024.
[23] Stewart, J.J.P. (1990) QCPE #455SGRW.
[24] CSD, Cambridge Crystallographic Data Centre, Cambridge.
[25] Beeman, D. (1976) J. Comp. Phys. 20, 130–139.
[26] Sugawara, M., Iseki, K., Miyazaki, K., Shiroto, H., Kondo, Y. and Uchino, J. (1991) J. Pharm. Pharmacol. 43, 882–884.
[27] Dantzig, A.H., Tabas, L.B. and Bergin, L. (1992) Biochim. Biophys. Acta 1112, 167–173.
[28] Yee, S. and Amidon, G.L. (1991) Pharm. Res. 8, S–198.
[29] Stein, W.D. (1990) Channels, carriers, and pumps. An introduction to membrane transport, pp. 127–171, Academic Press, San Diego.